



**HAL**  
open science

# Preparation and Photoluminescence Properties of Eu<sup>2+</sup>-Doped Oxyapatite-Type Sr<sub>x</sub>La<sub>10-x</sub>(SiO<sub>4</sub>)<sub>6</sub>O<sub>3-x/2</sub>

Cui Zhao-Feng, Yuan Shuang-Long, Yang Yun-Xia, François Cheviré, Franck Tessier, Chen Guo-Rong

► **To cite this version:**

Cui Zhao-Feng, Yuan Shuang-Long, Yang Yun-Xia, François Cheviré, Franck Tessier, et al.. Preparation and Photoluminescence Properties of Eu<sup>2+</sup>-Doped Oxyapatite-Type Sr<sub>x</sub>La<sub>10-x</sub>(SiO<sub>4</sub>)<sub>6</sub>O<sub>3-x/2</sub>. Chinese Physics Letters, 2011, 28 (1), pp.014209. 10.1088/0256-307X/28/1/014209 . hal-00854467

**HAL Id: hal-00854467**

**<https://hal.science/hal-00854467v1>**

Submitted on 9 Nov 2020

**HAL** is a multi-disciplinary open access archive for the deposit and dissemination of scientific research documents, whether they are published or not. The documents may come from teaching and research institutions in France or abroad, or from public or private research centers.

L'archive ouverte pluridisciplinaire **HAL**, est destinée au dépôt et à la diffusion de documents scientifiques de niveau recherche, publiés ou non, émanant des établissements d'enseignement et de recherche français ou étrangers, des laboratoires publics ou privés.

# Preparation and Photoluminescence Properties of $\text{Eu}^{2+}$ -Doped Oxyapatite-Type $\text{Sr}_x\text{La}_{10-x}(\text{SiO}_4)_6\text{O}_{3-x/2}$

Zhao-Feng CUI<sup>1</sup>, Shuang-Long YUAN<sup>1,2\*\*</sup>, Yun-Xia YANG<sup>1</sup>, François CHEVIRE<sup>2\*\*</sup>, Franck TESSIER<sup>2</sup>, Guo-Rong CHEN<sup>1</sup>

<sup>1</sup>Key Laboratory for Ultrafine Materials of Ministry of Education, School of Materials Science and Engineering, East China University of Science and Technology, Shanghai 200237

<sup>2</sup>UMR CNRS 6226 Sciences Chimiques de Rennes, équipe Verres et Céramiques, Université de Rennes 1, 35042 Rennes cedex, France

\*\* Email: shuanglong@ecust.edu.cn; francois.chevire@univ-rennes1.fr

*$\text{Eu}^{2+}$ -doped oxyapatite  $\text{Sr}_x\text{La}_{10-x}(\text{SiO}_4)_6\text{O}_{3-x/2}$  phosphors are prepared by solid-state reaction at high temperatures under reducing atmosphere. Their crystal structures and photoluminescence are investigated by x-ray diffraction (XRD) and fluorescence spectroscopy, respectively. The XRD results indicate that the samples are pure oxyapatite phase ( $P6_3/m$  space group). The fluorescence spectra show two peaks corresponding to two sites (4*f* and 6*h* sites) for  $\text{Eu}^{2+}$  in the host lattice. As the  $\text{Eu}^{2+}$  content influences the intensity ratio of the two observed emission peaks, the photoluminescence mechanism is discussed.*

Alkaline earth-rare earth silicates with the general formula  $\text{M}_x\text{Ln}_{10-x}(\text{SiO}_4)_6\text{X}$  ( $\text{M}=\text{Ca}, \text{Sr}, \text{Ba} \dots$ ;  $\text{Ln} = \text{La}, \text{Y}, \text{Gd} \dots$ ;  $\text{X} = \text{O}, \text{S}, \text{Se} \dots$ ) and the oxyapatite structure have been extensively studied for their high chemical and physical stabilities. This oxyapatite structure, in which the isolated covalent silicate tetrahedrons form the skeleton of the framework, contains two cationic sites that are the 9-fold coordinated 4*f*(I) site and 7-fold coordinated 6*h*(II) site. Cations occupying the latter site form tunnels for the X anions.<sup>[1]</sup> Such materials are usually used as oxide ion conductors for solid oxide fuel cells due to their good ionic conductivity.<sup>[2]</sup> In regards to their stable crystal structure and high thermal stability, they have also been used as host materials for phosphors doped with trivalent rare earth ions such as  $\text{Eu}^{3+}$ ,  $\text{Tb}^{3+}$ ,  $\text{Sm}^{3+}$ , and show excellent luminescent behaviors.<sup>[3-6]</sup>

As reported in the literature,  $\text{Eu}^{2+}$  is often used as a luminescent center as its emission and excitation spectra usually consist of broad bands due to electronic transitions between the  $^8S_{7/2}$  (4*f*<sup>7</sup>) ground state and the 4*f*<sup>6</sup>5*d* excited state.<sup>[7]</sup> Because the involved 5*d* orbitals are not shielded, they strongly depend on the host matrix,<sup>[8]</sup> consequently the excitation and emission bands are largely influenced by the environment of  $\text{Eu}^{2+}$  ions in the crystal structure, i.e. covalence, crystal field effect, bond lengths, symmetry and so on. Silicate phosphors activated by  $\text{Eu}^{2+}$  have usually been used as the phosphor for white light-emitting-diodes illumination due to a wide emission band under near ultraviolet and/or blue irradiation.<sup>[9]</sup> In particular, in alkaline earth-rare earth ternary silicate oxyapatites,  $\text{Eu}^{2+}$  can occupy

two different crystallographic sites which might result in excellent photoluminescence properties. However, the photoluminescence characteristics of  $\text{Eu}^{2+}$  doped silicate phosphors of the oxyapatite-type have been scarcely reported so far.

Thus, in the present work,  $\text{Eu}^{2+}$  doped  $\text{Sr}_x\text{La}_{10-x}(\text{SiO}_4)_6\text{O}_{3-x/2}$  (SLSOE) phosphors are prepared by solid state reaction at high temperature under reductive atmosphere, and their luminescent properties are investigated in detail.

Powder samples with the general formula  $\text{Sr}_{x-y}\text{La}_{10-x}(\text{SiO}_4)_6\text{O}_{3-x/2}:\text{Eu}_y$  were prepared by using  $\text{SrCO}_3$ (3N),  $\text{La}_2\text{O}_3$ (4N),  $\text{SiO}_2$ (4N) and  $\text{Eu}_2\text{O}_3$ (4N) as raw materials. After stoichiometric ratios of the starting materials were thoroughly mixed and ground in an agate mortar, the mixtures were pressed to form pellets and then fired at 1400°C for 6 h under reducing atmosphere ( $\text{N}_2 + \text{H}_2$  (10%)).

Sample purity of the prepared products was determined by powder x-ray diffraction (D8 ADVANCE, Bruker) using  $\text{Cu } K\alpha$  ( $\lambda = 1.5405 \text{ \AA}$ ) at room temperature. A spectrofluorometer (Fluorolog-3-P, Jobin Yvon) equipped with 450 W Xe-arc lamp was used for the photoluminescence measurement at room temperature. XRD patterns of  $\text{Sr}_x\text{La}_{10-x}(\text{SiO}_4)_6\text{O}_{3-x/2}:\text{Eu}^{2+}$  samples with  $x = 1$  to  $x = 5$  are gathered in Fig. 1 and show that the diffraction peaks are in good agreement with those of  $\text{Ca}_2\text{La}_8(\text{SiO}_4)_6\text{O}_2$  (JCPDS No.29-337), which are attributed to the hexagonal crystal form of oxyapatite based on the space group  $P6_3/m$ . All the samples are single phase, except for the sample  $x = 5$  in which some unknown peaks are observed. With the increasing  $x$  value, the reflections slightly shift to lower angles as a

consequence of a higher concentration of  $\text{Sr}^{2+}$  which ionic radius is larger than that of  $\text{La}^{3+}$ , i.e. 0.112 nm and 0.106 nm, respectively.

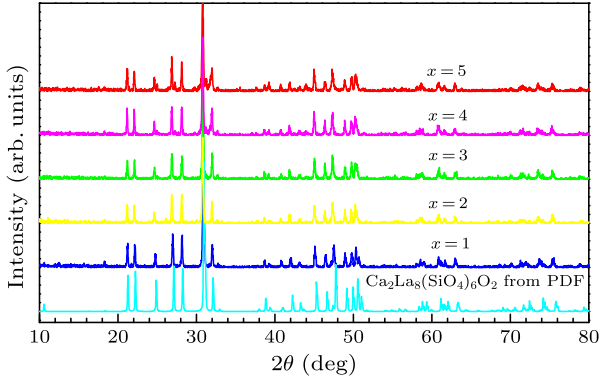


**Fig. 1.** X-ray diffraction patterns of  $\text{Sr}_x\text{La}_{10-x}(\text{SiO}_4)_6\text{O}_{3-x/2}:\text{Eu}^{2+}$ .

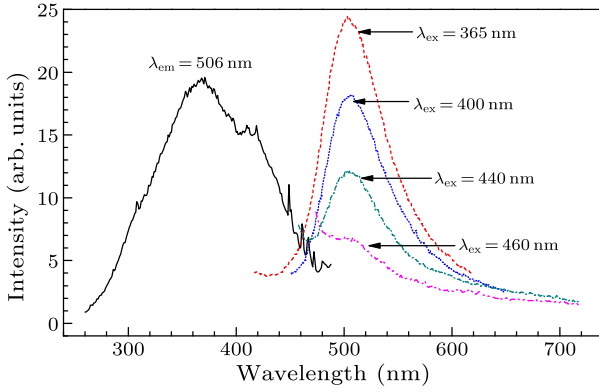


**Fig. 2.** Excitation and emission spectra of  $\text{Sr}_{1.95}\text{La}_8(\text{SiO}_4)_6\text{O}_2:\text{Eu}_{0.05}^{2+}$ .

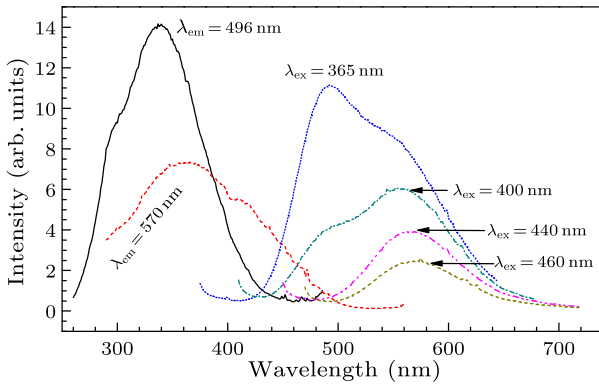


**Fig. 3.** Excitation and emission spectra of  $\text{Sr}_{3.95}\text{La}_6(\text{SiO}_4)_6\text{O}:\text{Eu}_{0.05}^{2+}$ .

Figures 2 and 3 show the excitation and emission spectra of  $\text{Sr}_{1.95}\text{La}_8(\text{SiO}_4)_6\text{O}_2:\text{Eu}_{0.05}^{2+}$  ( $x = 2$ ) and  $\text{Sr}_{3.95}\text{La}_6(\text{SiO}_4)_6\text{O}:\text{Eu}_{0.05}^{2+}$  ( $x = 4$ ), respectively. In the two cases, both excitation and emission bands are very broad. Especially for  $x = 4$ , the excitation band monitored at 570 nm even covers the range from 300 nm to 450 nm which matches well with the NUV/Blue

light emitting diodes (LEDs). The emission bands generally range from 420 nm to 650 nm and can be assigned to the  $4f^65d^1 \rightarrow 4f^7$  transition of  $\text{Eu}^{2+}$ . The characteristic sharp peaks of  $\text{Eu}^{3+}$  originating from the  $^5D - ^7F$  transitions are not observed,<sup>[10]</sup> thus we can assume that all  $\text{Eu}^{3+}$  ions have been reduced to  $\text{Eu}^{2+}$  during the synthesis. Moreover, PL spectra in Figs. 2 and 3 exhibit different behaviors, depending on Sr/La ratio or excitation wavelengths, which will be discussed later.

Figures 4(a) and 4(b) presents the photoluminescence spectra (PL) of  $\text{Sr}_{x-0.05}\text{La}_{10-x}(\text{SiO}_4)_6\text{O}_{3-x/2}:\text{Eu}_{0.05}$  samples ( $x = 0.05, 1, 2, 3, 4$  and  $5$ ) under excitation at 365 nm and 440 nm, respectively. Under excitation at 365 nm for  $x \leq 2$ , the emission band peaking around 510 nm seems to be unique. However, when  $x > 2$ , a shoulder appears at longer wavelengths and the band splits into two bands at about 496 nm and 566 nm. However when exciting at 440 nm, the  $x$  value has no influence on the symmetry of the emission band but changes its position, that is, if  $x \leq 2$ , emission at 490 nm dominates while if  $x > 2$ , emission at 566 nm occurs.

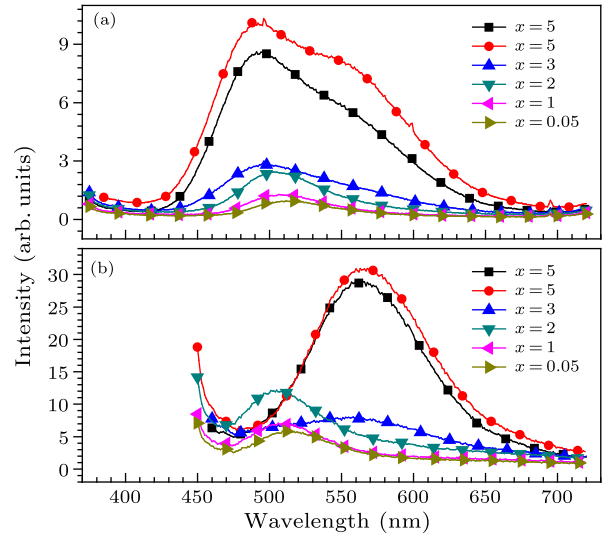


**Fig. 4.** Photoluminescence spectra of  $\text{Sr}_{x-0.05}\text{La}_{10-x}(\text{SiO}_4)_6\text{O}_{3-x/2}:\text{Eu}_{0.05}^{2+}$  ( $x = 0.05, 1, 2, 3, 4, 5$ ) excited at (a) 365 nm and (b) 440 nm.

As previously reported,<sup>[4]</sup> there are two sites for cations in the alkaline earth–rare earth silicate oxyapatite structure: a nine-coordinated site  $4f$  (I) with relatively longer bond lengths of cation-O, and a seven-coordinated site  $6h$  (II) with shorter bond lengths of cation-O. As mentioned above, the difference between the two sites is that the cation at  $6h$  site is coordinated to channel oxygen that is called the “free oxygen ion”. This oxygen atom does not belong to any anionic group while the nine oxygen ions coordinated to the  $4f$  site are all the members of the anionic group. This difference causes the atom at  $6h$  site to have a

higher covalency than that at  $4f$  site. As commonly admitted,  $\text{Eu}^{2+}$  at higher covalent site shows longer emission and excitation wavelength.<sup>[11]</sup> According to Ouenzerfi *et al.*,<sup>[12]</sup> in the oxyapatite structure, the six  $6h$  site will first be occupied by trivalent cation, then by other cation, which means that in the present case,  $\text{La}^{3+}$  first occupies the  $6h$  sites when  $x \leq 2$ , leaving behind  $4f$  sites for  $\text{Eu}^{2+}$  and  $\text{Sr}^{2+}$ . As a result, only one peak in the PL spectra is observed. However, as the content of  $\text{La}^{3+}$  decreases ( $x > 2$ ), some  $\text{Eu}^{2+}$  occupy the  $6h$  sites leading to two emission peaks in the PL, as shown in Figs. 4. Therefore, we can deduce that the short- and long-wavelength emissions are attributed to  $\text{Eu}^{2+}$  ions occupying the  $4f$  (I) and  $6h$  (II) cation sites respectively. Figures 2 and 3 can illustrate this conclusion as only one emission peak at 506 nm is observed for  $\text{Sr}_{1.95}\text{La}_8(\text{SiO}_4)_6\text{O}_2:\text{Eu}_{0.05}^{2+}$ , which is independent of the excitation wavelength, while for  $\text{Sr}_{3.95}\text{La}_6(\text{SiO}_4)_6\text{O}:\text{Eu}_{0.05}^{2+}$  two peaks appear as the excitation wavelength changes.

In addition, the emission intensity of  $\text{Sr}_{x-0.05}\text{La}_{10-x}(\text{SiO}_4)_6\text{O}_{3-x/2}:\text{Eu}_{0.05}$  phosphors basically increases with the increasing  $x$  value. This can also be explained by the distribution of the divalent europium in the available sites in the oxyapatite structure. In the case of  $x \leq 2$  where only one crystallographic site is offered for  $\text{Eu}^{2+}$ , all  $\text{Eu}^{2+}$  ions occupy the  $4f$  sites, leading to the high local  $\text{Eu}^{2+}$  concentration and resulting in concentration quenching. On the contrary for  $x > 2$ , the emission intensity increases remarkably. This can be demonstrated by the PL spectra of  $\text{Sr}_{4-y}\text{La}_6(\text{SiO}_4)_6\text{O}:\text{Eu}_y^{2+}$  with different  $\text{Eu}^{2+}$  concentrations (see Fig. 5).

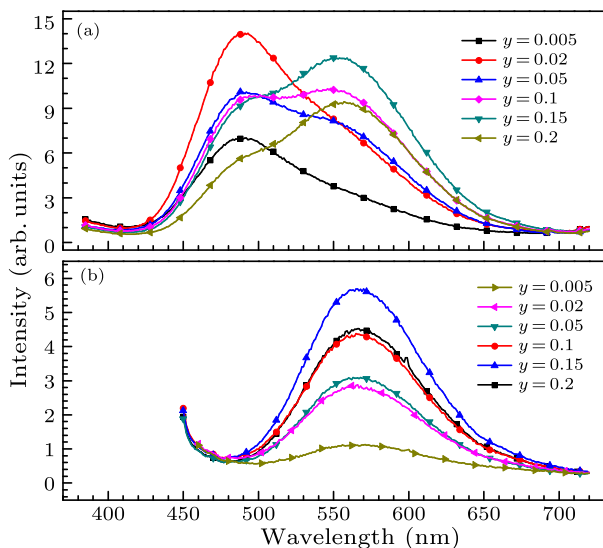


**Fig. 5.** (a) Photoluminescence spectra of  $\text{Sr}_{4-y}\text{La}_6(\text{SiO}_4)_6\text{O}:\text{Eu}_y^{2+}$  ( $y = 0.005, 0.02, 0.05, 0.1, 0.15, 0.2$ ) excited at (a) 365 nm and (b) 440 nm.

Moreover, as the  $x$  value increases, the emission peak around 510 nm shifts to a shorter wavelength

( $\sim 496$  nm). This can be explained by the change of the  $\text{Eu}(\text{I})\text{-O}$  bond length in the oxyapatite crystal structure as the shorter the bond length of covalent bond, the longer wavelength emission.<sup>[4]</sup> In the present experiments, more strontium atoms are introduced to the  $4f$  sites, resulting in a distorted crystal structure due to a larger ions radius of  $\text{Sr}^{2+}$  ions compared to that of  $\text{La}^{3+}$ . As a consequence, the  $\text{Sr}(\text{I})\text{-O}$  bond length increases. In  $\text{Sr}_2\text{La}_8(\text{SiO}_4)_6\text{O}_2$ , the  $\text{Sr}(\text{I})\text{-O}$  bond length is 2.548 Å while it is 2.569 Å in  $\text{Sr}_{3.1}\text{La}_{6.9}(\text{SiO}_4)_6\text{O}$ ,<sup>[13]</sup> these data are relevant with the above explanations on emission peak shifting observed for our samples.

The effect of  $\text{Eu}^{2+}$  doping concentration on the emission intensity of  $\text{Sr}_{4-y}\text{La}_6(\text{SiO}_4)_6\text{O}:\text{Eu}_y^{2+}$  with variation of the activator concentration ( $y = 0.005, 0.02, 0.05, 0.10, 0.15$  and  $0.20$ ) was also investigated. Figure 5 presents their emission spectra at 365 and 440 nm excitations, respectively. It can be observed that under excitation at 365 nm, the emission spectra are asymmetric broad bands. These asymmetric bands can be well decomposed into two Gaussian profiles peaking at about 484 and 545 nm, respectively. The detailed fitted data are listed in Table 1. According to the conclusion aforementioned, the short- and long-wavelength emission bands attribute to  $\text{Eu}(\text{I})$  and  $\text{Eu}(\text{II})$  respectively, and their integrated intensities labeled as A1 and A2 are also shown in Table 1. When  $\text{Eu}^{2+}$  ion concentration is lower ( $y \leq 0.05$ ), the short-wavelength emission at 484 nm predominates. With the increasing  $\text{Eu}^{2+}$  ion concentration, long-wavelength emission at 545 nm dominates progressively. However, all the PL spectra show single peak at 566 nm with good symmetry when excited by 440 nm.

Table 1. Fitted emission data of  $\text{Sr}_{4-y}\text{La}_6(\text{SiO}_4)_6\text{O}:\text{Eu}_y^{2+}$ .

$y$	0.005	0.02	0.05	0.10	0.15	0.20
$\lambda_{\text{Eu}(\text{I})}$	484	484	483	482	483	481
$\lambda_{\text{Eu}(\text{II})}$	528	540	544	549	553	556
A2/A1	1.75	1.54	2.84	4.40	6.42	9.04

According to Fig. 5(a), the emission intensity at 484 nm increases and then decreases and the one around 545 nm increases with increasing  $\text{Eu}^{2+}$  concentration. This phenomenon can be explained by two possible mechanisms, one is  $\text{Eu}^{2+}$  concentration increasing at the corresponding crystallographic site, and the other one involves energy transfer process between two kinds of  $\text{Eu}^{2+}$ . As discussed above,  $\text{Sr}_{4y}\text{La}_6(\text{SiO}_4)_6\text{O}:\text{Eu}_y$  have two crystallographic sites and divalent cation will firstly occupy  $4f$  site, therefore  $\text{Eu}^{2+}$  is also introduced at  $4f$  sites in the process of crystal growth, as a result the concentration of  $\text{Eu}^{2+}$  at  $4f$  sites increases, leading to increase of the intensity of short wavelength emission. As  $\text{Eu}^{2+}$  concentration keeps increasing, more  $\text{Eu}^{2+}$  ions occupy  $6h$

sites, which results in enhancing long wavelength emission intensity. Based on this deduction, the emission of short wavelength should not decrease as  $y > 0.02$ , because the maximum  $\text{Eu}^{2+}$  concentration at  $4f$  sites is  $y = 0.05$  as pointed out above. Therefore, we can deduce that energy transfer between  $\text{Eu(I)}$  and  $\text{Eu(II)}$  occurs because of large overlap between the excitation spectra at 570 nm and the emission spectra excited by 365 nm as shown in Fig. 3. Thus, the emission intensity of short wavelength decreases sharply and the one at long wavelength increases.

Upon 440 nm excitation, only  $\text{Eu(II)}$  ions can be efficiently excited and show a symmetric emission band, indicating that  $\text{Eu(I)}$  is not excited under 440 nm and no energy transfer occurs between  $\text{Eu(I)}$  and  $\text{Eu(II)}$ . The emission intensity increases and then decreases with  $\text{Eu}^{2+}$  concentration increasing, implying that  $\text{Eu}^{2+}$  concentration at  $6h$  site increases, which is in agreement with the result discussed above. The optimized  $y$  value is 0.15, beyond this value concentration quenching occurs.

In summary,  $\text{Sr}_{x-y}\text{La}_{10-x}(\text{SiO}_4)_6\text{O}_{3-x/2}:\text{Eu}_y$  ( $x = 0.05, 1, 2, 3, 4, 5$ ;  $y = 0.005, 0.02, 0.05, 0.1, 0.15, 0.2$ ) phosphors have been synthesized by solid-state reaction at high temperature under reducing atmosphere. They exhibit wide excitation and emission bands, implying that these compositions can potentially be used as novel phosphors for white light emitting diodes. When  $x \leq 2$ , only one emission peak around 510 nm; however, with the increasing  $\text{Sr}^{2+}$  con-

centration, two peaks appear at 496 nm and 566 nm, which are ascribed to the emission of  $\text{Eu}^{2+}$  at  $4f$  and  $6h$  sites, respectively. The 510-nm emission peak shifts to 496 nm as a result of the Sr(I)-O bond length increase. For  $\text{Sr}_{4-y}\text{La}_6(\text{SiO}_4)_6\text{O}:\text{Eu}_y$  ( $y = 0.005, 0.02, 0.05, 0.1, 0.15, 0.2$ ), as the content of  $\text{Eu}^{2+}$  increases, the relative luminous intensity of 566–496 nm increases.

## References

- [1] Zhang J, Liang H, Yu R, Yuan H and Su Q 2009 *Mater. Chem. Phys.* **114** 242
- [2] Vincent A, Savignat S B and Gervais F O 2007 *J. Eur. Ceram. Soc.* **27** 1187
- [3] Lin Y, Tang Z, Zhang Z and Nan C W 2003 *J. Alloys Compd.* **348** 76
- [4] Lin J and Su Q 1994 *Mater. Chem. Phys.* **38** 98
- [5] Lin J and Su Q 1995 *J. Mater. Chem.* **5** 1151
- [6] Lin J and Su Q 1994 *J. Alloys Compd.* **210** 159
- [7] Dorenbos P 2003 *J. Lumin.* **104** 239
- [8] Fang Y, Zhuang W D, Cui X Z, Hu Y S and Huang X W 2006 *J. Rare Earths* **24** (Suppl. 1) 145
- [9] Zhang X M, Li W L and Seo H J 2009 *Phys. Lett. A* **373** 3486
- [10] Ouenzerfi R E, Goutaudier C, Cohen-Adad M T, Panczer G and Boulon G 2003 *J. Lumin.* **102–103** 426
- [11] Li Y, Chang Y, Tsai B, Chen Y and Lin Y 2006 *J. Alloys Compd.* **416** 199
- [12] Ouenzerfi R E, Panczer G, Goutaudier C, Cohen-Adad M T, Boulon G, Trabelsi-Ayedi M and Kbir-Arighuib N 2001 *Opt. Mater.* **16** 301
- [13] Seeta R R G, Jung H C, Park J Y, Moon B K, Balakrishnaiah R, Jeong J H and Kimb J H 2010 *Sensors Actuators B: Chem.* **146** 395